THE JOURNAL OF COMPARATIVE NEUROLOGY 500:239–254 (2007)

# Magnetic Resonance Imaging and Histological Studies of Corpus Callosal and Hippocampal Abnormalities Linked to *doublecortin* Deficiency

CAROLINE KAPPELER,[1–4] MARC DHENAIN,[5,6] FRANÇOISE PHAN DINH TUY,[1–4] YOANN SAILLOUR,[1–4] SERGE MARTY,[7] CATHERINE FALLET-BIANCO,[8] ISABELLE SOUVILLE,[9] EVELYNE SOUIL,[10] JEAN-MARC PINARD,[11] GUNDELA MEYER,[12] FERECHTÉ ENCHA-RAZAVI,[13] ANDREAS VOLK,[5] CHERIF BELDJORD,[9] JAMEL CHELLY,[1–4] AND FIONA FRANCIS[1–4]*

[1]Département de Génétique et Développement, Institut Cochin, F-75014 Paris, France
[2]Institut National de la Santé et de la Recherche Médicale U567, Paris, France
[3]Centre National de la Recherche Scientifique UMR 8104, Paris, France
[4]Université René Descartes, Paris V, 75014 Paris, France
[5]U759 Institut National de la Santé et de la Recherche Médicale/Institut Curie, Centre Universitaire, Orsay, France
[6]URA CEA Centre National de la Recherche Scientifique 2210, SHFJ, 91401 Orsay, France
[7]Institut National de la Santé et de la Recherche Médicale U497, Ecole Normale Supérieure, 75005 Paris, France
[8]Service d'Anatomie Pathologique, Hôpital Sainte Anne, 75014 Paris, France
[9]Laboratoire de Biochimie Génétique, CHU Cochin Port Royal, 75014 Paris, France
[10]Laboratoire d'Anatomie Pathologie, Institut Cochin, 75014 Paris, France
[11]Unité de Neurologie pédiatrique, Hôpital Raymond Poincaré, 92380 Garches, France
[12]Department of Anatomy, Faculty of Medicine, University of La Laguna, La Laguna 39071, Tenerife, Spain
[13]Service d'Histologie Embryologie Cytogénétique, Groupe Hospitalier Necker-Enfants malades, 75015 Paris

ABSTRACT

Mutated *doublecortin* (*DCX*) gives rise to severe abnormalities in human cortical development. Adult *Dcx* knockout mice show no major neocortical defects but do have a disorganized hippocampus. We report here the developmental basis of these hippocampal abnormalities. A heterotopic band of neurons was identified starting at E17.5 in the CA3 region and progressing throughout the CA1 region by E18.5. At neonatal stages, the CA1 heterotopic band was reduced, but the CA3 band remained unchanged, continuing into adulthood. Thus, in mouse, migration of CA3 neurons is arrested during development, whereas CA1 cell migration is retarded. On the Sv129*Pas* background, magnetic resonance imaging (MRI) also suggested abnormal dorsal hippocampal morphology, displaced laterally and sometimes

This article includes Supplementary Material available via the Internet at http://www.interscience.wiley.com/jpages/0021-9967/suppmat.

Grant sponsor: Institut National de la Santé et de la Recherche Médicale; Grant sponsor: Centre National de la Recherche Scientifique; Grant sponsor: European Commission; Grant number: QLG3-CT-2000-00158.

*Correspondence to: Fiona Francis, Institut Cochin-CHU Cochin, 24 rue du Faubourg Saint Jacques, 75014 Paris, France.
E-mail: francis@cochin.inserm.fr

Received 9 January 2006; Revised 2 May 2006; Accepted 1 August 2006
DOI 10.1002/cne.21170
Published online in Wiley InterScience (www.interscience.wiley.com).

rostrally and associated with medial brain structure abnormalities. MRI and cryosectioning showed agenesis of the corpus callosum in *Dcx* knockout mice on this background and an intermediate, partial agenesis in heterozygote mice. Wild-type littermates showed no callosal abnormalities. Hippocampal and corpus callosal abnormalities were also characterized in *DCX*-mutated human patients. Severe hippocampal hypoplasia was identified along with variable corpus callosal defects ranging from total agenesis to an abnormally thick or thin callosum. Our data in the mouse, identifying roles for Dcx in hippocampal and corpus callosal development, might suggest intrinsic roles for human DCX in the development of these structures. J. Comp. Neurol. 500:239–254, 2007. 

**Indexing terms: Dcx; hippocampal heterotopia; agenesis of the corpus callosum; human cortical malformation**

The human *doublecortin* (*DCX*) gene is mutated in type I lissencephaly and subcortical laminar heterotopia (SCLH; des Portes et al., 1998a; Gleeson et al., 1998). A severely disorganized neocortex is the major anatomical modification in these disorders. The origin of these abnormalities, as well as their relationship with other brain alterations, is still poorly understood. *Dcx* knockout mice show no major anatomical differences in the neocortex compared with wild-type mice (Corbo et al., 2002; Kappeler et al., 2006). BrdU labeling studies thus showed that radial migration in the neocortex occurs relatively normally in these animals. Abnormalities have, however, subsequently been detected in populations of tangentially migrating interneurons derived from the ganglionic eminence during development and the adult subventricular zone (Kappeler et al., 2006; Koizumi et al, 2006a). These latter studies illustrate that *Dcx* knockout mice, although not fully mimicking the human disorder, can be used to provide further hints of Dcx's function.

*Dcx* knockout mice, despite the lack of major neocortical abnormalities, were shown to have a disorganization of the CA3 region in the adult hippocampus (Corbo et al., 2002). The developmental origin of these abnormalities was not, however, investigated in this study. Indeed, *Dcx* knockout mice provide a unique opportunity for assessing the role of mouse Dcx in hippocampal development in the absence of major neocortical abnormalities. Human hippocampal abnormalities specifically identified in cases of type I lissencephaly are rarely described in the literature (Forman et al., 2005; Montenegro et al., 2006). It is generally believed that the severe disorganization of the neocortex is likely to be associated with abnormalities in the hippocampus, but some studies have suggested that the hippocampus can be completely normal in these cases (Forman et al., 2005). We were therefore interested in better understanding the role of both mouse and human Dcx/DCX in hippocampal development.

A double-knockout of *Dcx* and a homologous gene, *doublecortin-like kinase 1* (*Dclk1*), has also recently been performed (Koizumi et al., 2006b; Deuel et al., 2006). These mice show radial migration abnormalities in the neocortex, suggesting that Dclk1 compensates for Dcx in the single knockout. The double-knockout mice also show severe corpus callosal defects, suggesting a role for this family of proteins in callosal axon growth or guidance. An appreciable proportion of human type I lissencephaly patients have also been reported to have corpus callosal abnormalities (Dobyns et al., 1999), although it has remained unclear whether these are directly correlated with the severe neocortical abnormalities.

In this study, we further characterized anatomical alterations in our single-knockout *Dcx* mouse model (Kappeler et al., 2006). Mice were crossed and evaluated on two pure backgrounds (C57BL/6N and Sv129*Pas*) to reveal defects modified by the genetic environment (Banbury Conference, 1997). This study was based on histological analyses of animals and magnetic resonance microimaging (μMRI), which allowed us to perform three-dimensional (3D) representations of mutant and wild-type brains and hence to evaluate accurately the malformations identified. In a complementary aspect of this study, we evaluated *DCX*-mutated patients, focusing on alterations that were highlighted in *Dcx* mutant mice. Our combined data support a role for DCX/Dcx in hippocampal as well as corpus callosal development, fitting with its function as a widely expressed, neuronal microtubule-associated protein (Francis et al., 1999; Gleeson et al., 1999; Horesh et al., 1999).

## MATERIALS AND METHODS

### Mice

*Dcx* knockout mice (deleted for *Dcx* exon 3) were generated by using the Cre-loxP site-specific recombination system, as described elsewhere (Kappeler et al., 2006). *Dcx* is present on the X chromosome, so male hemizygote mutant mice have no functional Dcx protein (Kappeler et al., 2006). Hemizygote and heterozygote *Dcx* mutant mice were crossed onto C57BL/6N and Sv129*Pas* backgrounds for at least five generations (Banbury Conference, 1997). No major differences were observed between hemizygote males and homozygote females. For most of the analyses described here, male hemizygous knockout mice were compared with littermate male wild-type mice or female heterozygotes. These animals were generated in most cases with wild-type littermate controls by crossing heterozygote females with pure C57BL/6N or Sv129*Pas* males (Charles River France). Hybrid background mice (F1) were generated by crossing female heterozygotes on the Sv129*Pas* background with male C57BL/6N wild-type mice. Mice were genotyped at postnatal day 10 (P10) or at embryonic stages by either Southern blotting or PCR, following standard methods (Sambrook et al., 1989). Experiments involving mice were performed by authorized investigators following national ethical guidelines.

## Western blots and immunodetections

To assay Dcx in postnatal stages, protein extracts were prepared from P4, P10, P22, and P30 brains and analyzed by SDS-PAGE and Western blotting, following standard procedures (Sambrook et al., 1989). Antibodies directed against Dcx (Nterm; Francis et al., 1999; 1:5,000) and α-tubulin (Sigma; 1:10,000) were used for immunodetection.

## BrdU labeling and immunohistochemistry

Embryos were collected from timed-pregnant females (where E0.5 is the day of detection of the vaginal plug). Alternatively, newborn or adult mice were sacrificed and the brains recovered for analysis. Brains were either frozen directly in isopentane or first fixed in 4% (w/v) paraformaldehyde (PFA) and cryoprotected in 10% (w/v) sucrose in phosphate buffer (pH 7.4) prior to freezing. Ten-micrometer serial sections were obtained with a Leica CM3050S cryostat. Neuronal progenitor cells of embryos at different stages of development were labeled in vivo by intraperitoneal injections of timed-pregnant females with bromodeoxyuridine (BrdU; 150 μg/g body weight). Females were sacrificed and embryos recovered at different times after injection ranging from 30 minutes to several days. Immunodetection was performed with anti-BrdU (Becton Dickinson; 1:25) or purified anti-Dcx (Nterm; Francis et al., 1999) and an ARK Peroxidase kit (DAKO), and sections were countercolored with Hemalun Mayer, followed by 10 mM ammonium acetate treatment.

## μMRI analysis

μMRI can be useful for evaluating complex 3D structures from intact samples without having to slice and reconstruct the samples (Dhenain et al., 2001). To perform this analysis, adult mice were killed by cervical dislocation, and their heads were fixed in 10% (v/v) buffered formalin for 1 week. Brains were then removed from the skulls and soaked in a 1:40 mixture of 0.5 mmol/ml gadoteric acid (Dotarem, Guerbet, France) and 10% (v/v) buffered formalin. This protocol, called "passive staining," reduces the T1, T2, and T2* relaxation times in brain tissues and augments the contrast-to-noise ratio between white and gray matter (Dhenain et al., 2006). After 1 week, brains were embedded in 2.5% (w/v) agarose and imaged on a 4.7-T Bruker Biospec system with a surface coil actively decoupled from the transmitting birdcage probe. Three-dimensional gradient echo images were recorded with the following parameters: TR = 100 msec, TE = 15 msec, alpha = 90°, field of view = $1.6 \times 1.2 \times 0.75$ cm$^3$, matrix = $256 \times 256 \times 128$, resolution = $62.5 \times 46.8 \times 58.6$ μm$^3$, NA = 10, imaging time = 9 hours. Images were zero-filled to reach an apparent resolution of $62.5 \times 46.8 \times 29.3$ μm$^3$. The matrices from each animal were rotated according to the X, Y, and Z direction to ensure that brains were positioned similarly before being analyzed (code developed under IDL5.5; Research Systems Inc.).

Most morphological analyses were performed from the zero-filled 3D matrices in AMIRA 3.1 (Mercury Computer Systems, Inc., TGS Unit, Villebon, France). The border of the brain was drawn at the pial surface (excluding olfactory bulbs and cerebellum, as described by Delatour et al., 2006). The first and last brain slices corresponded, respectively, to the most anterior part of the frontal pole and the most posterior part of the occipital cortex. The length of the anterior-posterior axis of each brain was defined by counting the number of sections between these two slices and then multiplying by 62.5 μm (μMRI slice thickness). The hippocampus was drawn at the gray/white matter border with the fimbria/corpus callosum. Hippocampal and brain volumes were calculated in AMIRA. In addition, hippocampal and brain coronal, horizontal, and sagittal profiles were drawn by calculating the surface of each brain slice in a given direction. The length of the corpus callosum was measured in DISPLAY freeware (ftp.bic.mni.mcgill.ca). In this case, a starting point was placed at the most rostral position of the genu of the corpus callosum, where white matter appeared continuous across the midline. A finishing point was placed at the most caudal position of the splenium of the corpus callosum, where white matter last appears continuous. The length of the line between these two points was used to determine the corpus callosum length. The length of the cerebral hemispheres for each brain was similarly assessed, as was the position of the anterior commissure with respect to the beginning of the hemispheres. μMRI data is available upon request.

## Neuropathological analyses of human fetal brain

Neuropathological studies were performed in three fetuses aged 35–36 gestational weeks (GW) after spontaneous abortions or pregnancy termination for fetal malformations, in accordance with French and Spanish legislation. After 10% (v/v) formalin with 0.3% (w/v) zinc sulfate or Bouin's fixation, brains were embedded in paraffin and cut into series of 10-μm-thick sections. Sections were Nissl stained to reveal the hippocampus and corpus callosum.

## Photomicrograph production

Photomicrographs were acquired with either a Nikon SMZ 1500 focusing telescope or a Nikon Eclipse E800 microscope, equipped with a DXM 1200F digital camera and ACT-1 software (Nikon France S.A., Champigny Sur Marne, France). MRI data, visualized in DISPLAY freeware (ftp.bic.mni.mcgill.ca) or AMIRA 3.1, were captured with a screen-capture tool (Screenshot; http://www.x-shot.de). Photomicrographs were manipulated in Adobe Photoshop 7.0.1 and figures were assembled in Microsoft Powerpoint. Contrast and brightness of photomicrographs were adjusted in either Powerpoint (Fig. 1) or Photoshop (Figs. 2–9, Supplementary Figs. 1–7), with knockout and wild-type images in multipart figures receiving similar treatments. These treatments were as follows: Figure 1, brightness 44–68%, contrast 47–74%; Figure 2, brightness +10, contrast +40; Figure 3, brightness +30; Figure 4, no treatments; Figure 5, contrast +70; Figure 6, contrast +60; Figure 7, brightness +20, Figure 8A–C, brightness +10, contrast +50; Figure 8D–F, brightness +20, contrast +5; Figure 9A–C, brightness +30, contrast +45; Figure 9D,E, brightness +10, contrast +10; Supplementary Figure 1, background subtraction using Image J (NIH; rolling ball radius 50), contrast +50; Supplementary Figure 2, contrast +30; Supplementary Figure 3, contrast +40; Supplementary Figure 4, brightness +40, contrast +20; Supplementary Figure 5, brightness +20, contrast +5; Supplementary Figure 6, brightness –10, contrast +60; Supplementary Figure 7, brightness –20, contrast +30.

# RESULTS

## Migration defects in the hippocampus of *Dcx* knockout embryos

We and others have already reported that no major radial migration defects could be detected in the neocortex of *Dcx* knockout mouse embryos (Corbo et al., 2002; Kappeler et al., 2006). Nevertheless hippocampal defects in the adult have previously been described (Corbo et al., 2002). We therefore decided to investigate the organization of the developing hippocampus in our mouse model, to search for defects in migrating hippocampal neurons. E14.5 and E16.5 male hemizygous mutant hippocampi displayed no major abnormalities compared with controls (data not shown). At E17.5, E18.5, and early postnatal stages, however, modifications were observed in mutant embryos on both C57BL/6N and Sv129*Pas* backgrounds. Specifically, knockout hippocampi exhibited an increased density of cells in the intermediate zone adjacent to the developing pyramidal cell layer (Fig. 1A–F, Supplementary Fig. 1A–C). At E17.5, two cell layers were observed in the CA3 region (Fig. 1A,B), tapering off in the CA1 region, whereas, at E18.5 and neonatal stages, a heterotopic band was also evident throughout the CA1 region (Fig. 1C–F). However, at these later stages, the proportion of heterotopic cells appeared diminished in the CA1 region and unchanged in the CA3 region (Supplementary Fig. 1). Thus, there is a temporal CA3 to CA1 gradient of heterotopic cells.

We further examined the nature of these cells by performing BrdU injections. First, an injection was performed at the peak of neurogenesis for radially migrating CA1 neurons (E15.5). Analysis of knockout animals killed at P1 showed an abnormal organization of BrdU-positive cells in the intermediate zone adjacent to the CA1 and CA3 regions as well as the presence of BrdU-positive cells throughout the normal pyramidal cell layer (Supplementary Fig. 1B). These data, and particularly the timing of the BrdU injection, are thus in keeping with radial migration defects in the hippocampus. Further confirmation was provided by BrdU labeling at E17.5 with death of embryos 30 minutes later, which showed no apparent proliferation abnormalities in the knockout brain (Supplementary Fig. 1C). Under these conditions, BrdU-labeled cells were observed almost exclusively in the ventricular zone and presumptive dentate gyrus and not in the heterotopic layer. These combined data confirm that the heterotopic layer of cells is formed from postmitotic radially migrating neurons, which may be retarded or arrested in their migration.

## Hippocampal abnormalities in adult *Dcx* knockout mice

We next examined the hippocampus in adult *Dcx* knockout mice. As previously reported by Corbo et al. (2002), the CA3 region was found to be disorganized. With our *Dcx* knockout mouse model analyzed on pure genetic backgrounds, we were able in particular to distinguish a clear division of the CA3 pyramidal cell layer into two distinct layers (Fig. 2A–D, Supplementary Fig. 2A–D). An intermediate phenotype was observed in female heterozygote mice (Supplementary Fig. 3). We systematically analyzed coronal sections histologically in eight knockout and eight wild-type animals on the Sv129*Pas* background, and the division of the pyramidal cell layer in the CA3 region was obvious in both rostral (Fig. 2A,B) and caudal (Fig. 2C,D) regions. These abnormalities in adulthood thus seem quite similar to the abnormally divided radially migrating cells observed in these animals during development, suggesting that heterotopic CA3 cells are arrested in their migration. Thus, certain migrating neurons destined for the CA3 region remain misplaced in adult life. Fewer abnormalities were observed in the CA1 region, although the pyramidal cell layer was slightly more diffuse than wild type, with sparse heterotopic cells found in the stratum oriens and in the subiculum (Fig. 2B). These data suggest that the majority of heterotopic neurons observed during development in the CA1 region seem likely to reach the pyramidal cell layer in neonatal and early postnatal stages. The dentate gyrus appeared largely normal in knockout animals by Nissl staining, although, interestingly, we have previously identified a disorganization of immature calretinin-positive granular cells in the superior blade of the dentate gyrus in adult animals (Kappeler et al., 2006). This disorganization seems, however, to have no major effect on dentate gyrus morphology.

Analysis of six wild-type and 10 knockout mice on the C57BL/6N background also showed two bands of pyramidal neurons in the knockout CA3 region at different rostrocaudal levels and sparse heterotopic cells in the CA1 region (Supplementary Fig. 2). The abnormalities were slightly milder than those observed on the Sv129*Pas* background, though always obvious to investigators blind to the genotypes. In addition, we observed similar abnormalities in female homozygote animals on the C57BL/6N background (Supplementary Fig. 4) and in knockout mice on the Sv129*Pas*/C57BL/6 F1 hybrid background (data not shown). Thus, a divided pyramidal cell layer in the CA3 region and only a very mildly disorganized CA1 region are consistently observed in *Dcx* knockout mice on defined genetic backgrounds.

## Hippocampal abnormalities in human patients

As with mouse Dcx, human DCX is expressed throughout the hippocampus during development (data not shown). We were therefore interested in comparing hippocampal defects in *DCX*-mutated patients with those observed in the mouse knockout. This is to our knowledge the first detailed anatomical description of hippocampal abnormalities in cases of *DCX*-mutated type I lissencephaly. We found, in three human fetal hippocampi (35–36 GW), that the entire Ammon's horn and the dentate gyrus were severely hypoplastic (Fig. 3). At this late prenatal stage, however, the human CA3 region did not seem to be more specifically affected than the rest of the Ammon's horn, and no heterotopic bands were observed (Fig. 3A–C). The severity of the hippocampal defects in these cases did not seem to be strictly correlated with the severity of the neocortex. Specifically, in two of three cases examined (case 148 in Fig. 3B and case 192, data not shown), relatively moderate hypoplasia of the CA1–CA3 region and the dentate gyrus was observed, whereas case 207 (Fig. 3C) showed an almost completely absent hippocampus, with a barely discernible dentate gyrus. However, both cases 148 and 207 have equally severe agyria. These data might therefore suggest a dissociation of DCX's function in the hippocampus from the neocortex. Human DCX is likely to be crucial for hippocampal development, in that

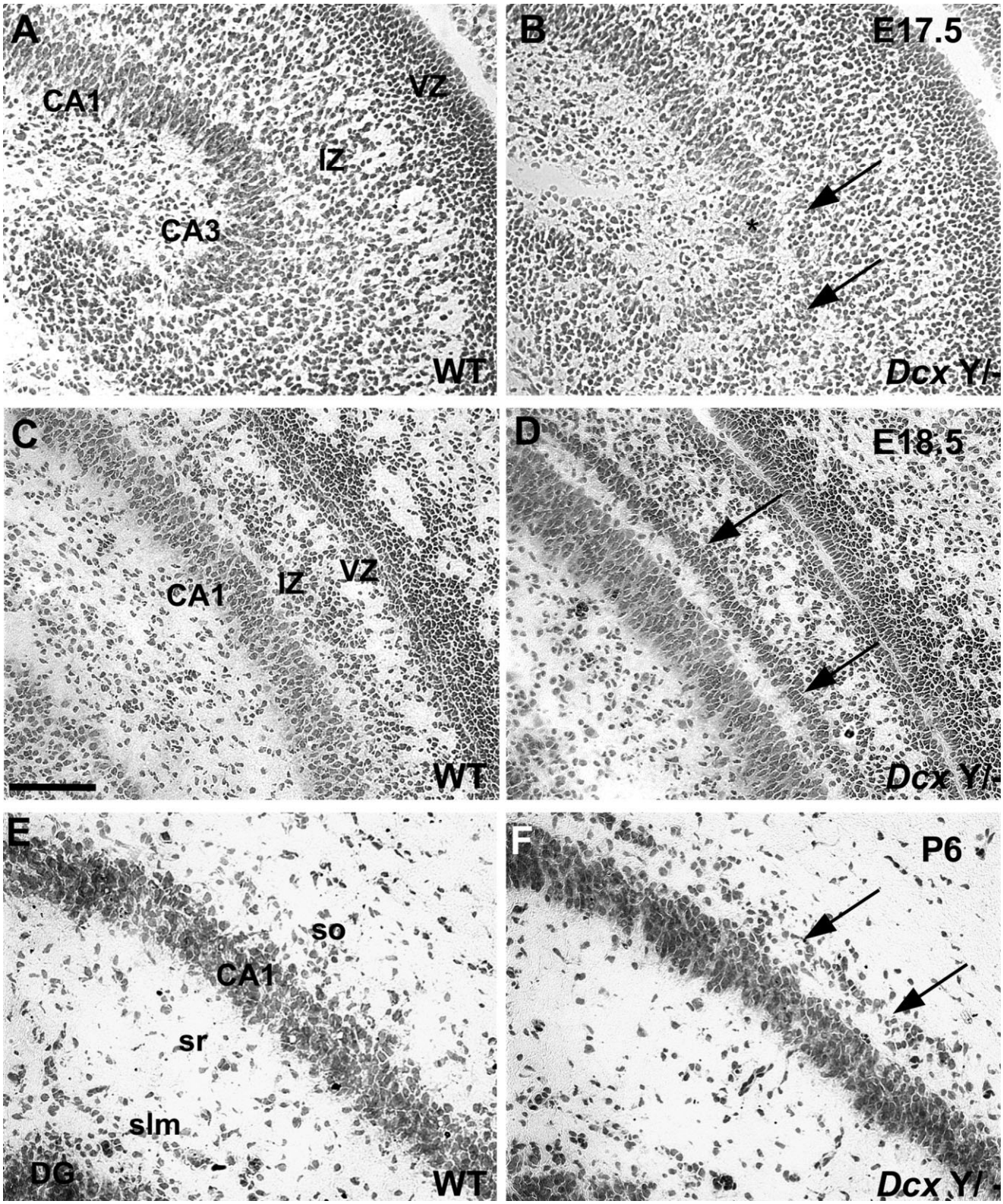


Fig. 1. Radial migration abnormalities in the embryonic and newborn hippocampus. A–F: Histologically stained sections show differences between wild-type (WT) and *Dcx* Y/– developing hippocampi. **A,B:** Cresyl violet-stained coronal sections at E17.5 show a heterotopic layer (arrows) in the CA3 region of the *Dcx* Y/– hippocampus. The asterisk denotes the continuous pyramidal cell layer. **C,D:** Hemotoxylin-eosin-stained coronal sections at E18.5 show an extensive heterotopic layer (arrows) in the upper part of the intermediate zone of the CA1 region. **E,F:** Cresyl violet-stained coronal sections at P6 show only a thin residual heterotopic band (arrows) in the medial part of the CA1 region. For each stage at least two mutant animals were examined. VZ, ventricular zone; IZ, intermediate zone; so, stratum oriens; sr, stratum radiatum; slm, stratum lacunosum moleculare; DG, dentate gyrus. Scale bar = 200 μm.

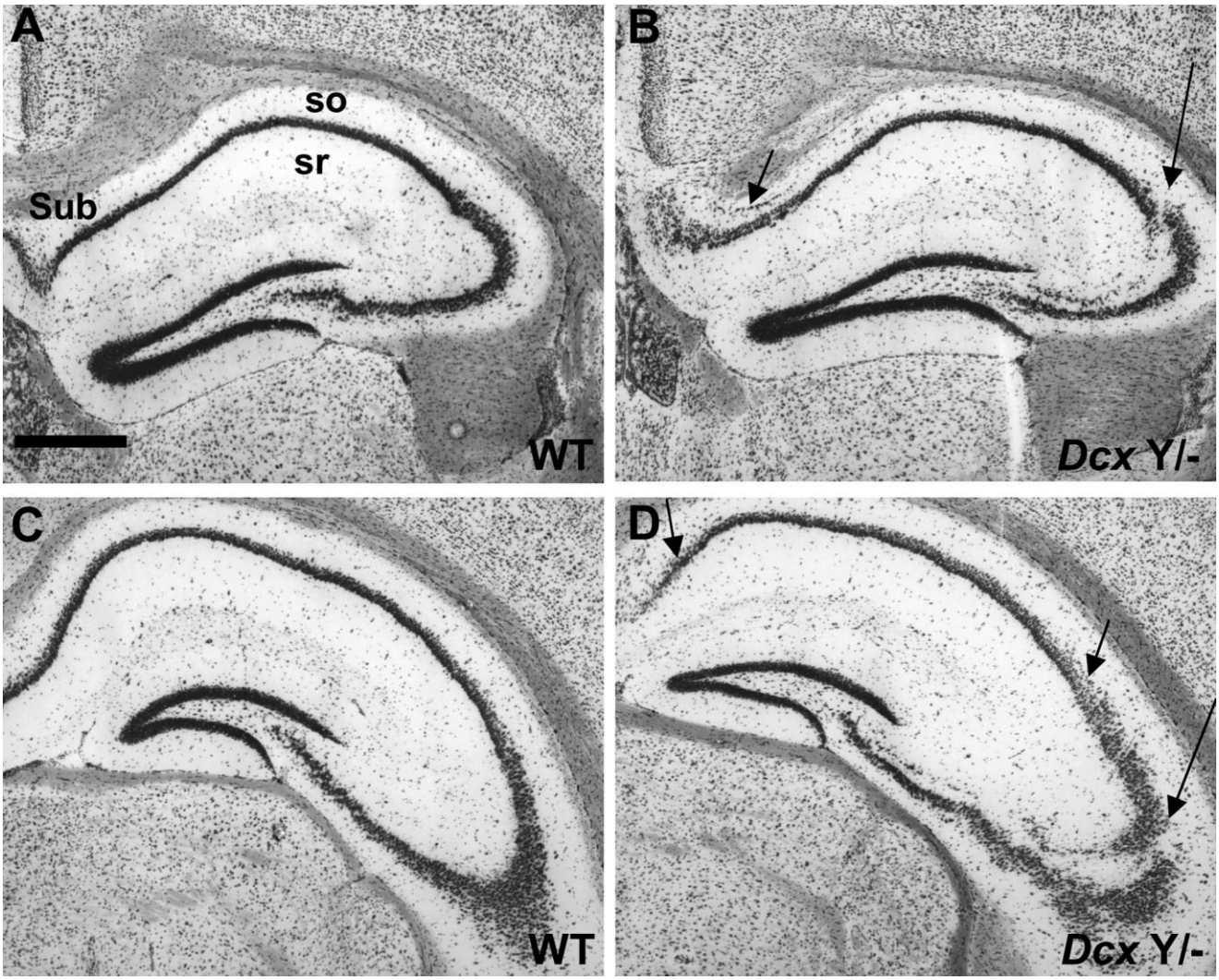


Fig. 2. Hippocampal abnormalities in adult Sv129*Pas* knockout mice. **A–D:** Cresyl violet/luxol blue-stained coronal sections of adult hippocampus from Sv129*Pas* control and *Dcx* Y/– mice showing a largely normal CA1 region but a disorganized CA3 region. This disorganization is characterized by two distinct pyramidal cell layers (long arrow) observed throughout the rostrocaudal extent of the hippocampus. Some residual heterotopic cells are observed more medially (short arrow, B) and the CA1 region in knockout animals was found to be slightly more diffuse (short arrows, D) and less well-organized compared with wild-type. Eight knockout and wild-type animals were examined on this background by cryosectioning, showing similar results. Sub, subiculum; so, stratum oriens; sr, stratum radiatum. Scale bar = 500 μm.

the human phenotype is clearly more dramatic than that in mouse.

## MRI studies of mouse hippocampi

The observation of severe hippocampal hypoplasia in human patients led us to reexamine hippocampal volume in *Dcx* mutant mice. Male knockout (n = 2) and wild-type (n = 2) littermate mouse brains from each genetic background were thus analyzed at high resolution by in vitro μMRI. A passive staining technique was used to increase the contrast between gray and white matter (Dhenain et al., 2006). CA3 region abnormalities were just visible with this technique (data not shown), although they could not be identified with as much accuracy as in the histological analyses. The μMRI data show that there is some variability of hippocampal volumes between the genetic backgrounds and between the genotypes. For age-matched animals on the C57BL/6N background, the mutant hippocampi appear slightly larger than wild-type hippocampi. On the other hand, on the Sv129*Pas* background, either the hippocampal volumes are identical between wild-type and mutant brains (Table 1; compare Sv129*Pas* WT1 vs. Sv129*Pas Dcx*Y/–1) or the mutant hippocampus is slightly smaller (Table 1; compare Sv129*Pas* WT2 vs. Sv129*Pas Dcx*Y/–2). Thus, it is not currently possible to draw any firm conclusions from these data concerning overall hippocampus volume in the mutant mouse, although it seems that no major hypo- or hyperplasia occurs, despite the migration abnormalities.

Our μMRI analyses in Sv129*Pas* animals suggested specific hippocampal abnormalities particular to this background. Initially, an assessment of hippocampal vol-

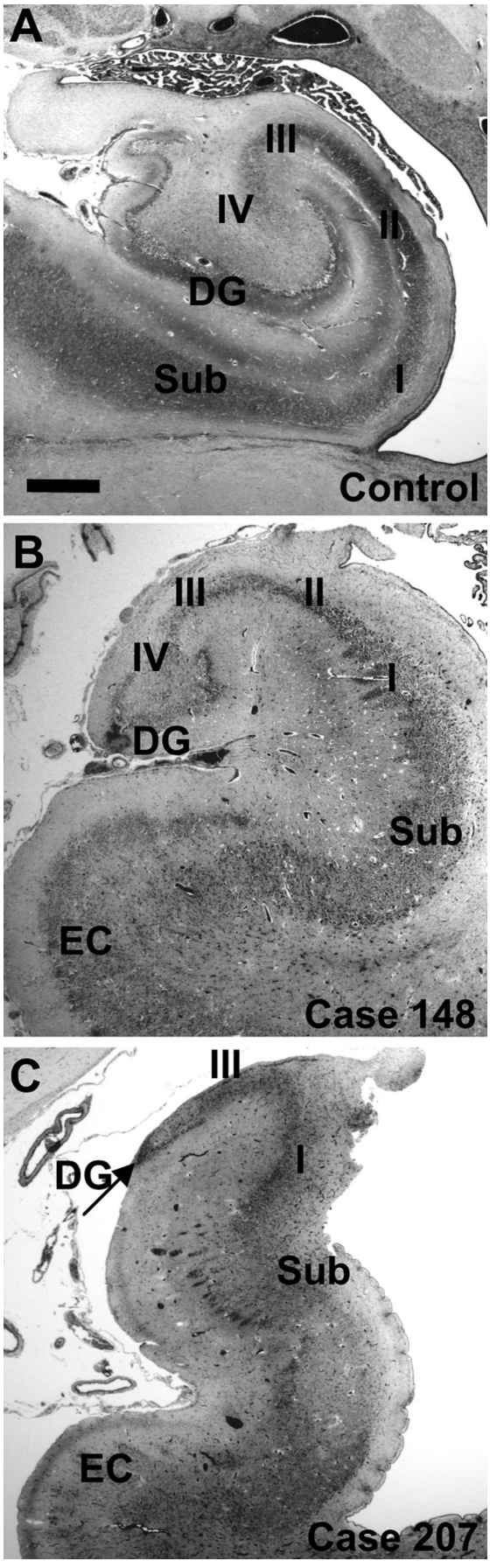


umes in individual μMRI slices showed differences in the two mutant animals analyzed compared with their age-matched controls (Fig. 4A, Supplementary Fig. 5). In both mutant animal brains analyzed, in a rostral to caudal direction, we observed that the slice volumes rise more slowly in the dorsal part of mutant hippocampi compared with controls. Such differences in volume were also obvious when comparing slice volumes in the sagittal plane (data not shown). At both ages examined (2 months and 13 months), mutant hippocampi showed similar alterations. A 3D representation summarizing these data shows that the less voluminous, dorsal part of the mutant hippocampus is in fact turned away from the midline in the Sv129*Pas Dcx* knockout animals (Fig. 4B,C, Supplementary Fig. 5A–F). Histological analyses in a larger number of mutant Sv129*Pas* animals suggested similar alterations (data not shown). We also observed in μMRI and histological studies that in certain animals (2/10 animals analyzed) the hippocampus and associated white matter tracts (hippocampal fimbria, dorsal fornix, and ventral hippocampal commissure) were positioned more rostrally with respect to the anterior commissure (Figs. 4A, 5A,B, Supplementary Figs. 5A–F, 6A–F; Bregma, 0.02–0.14 mm). Thus, both μMRI and histology show that the dorsal part of the knockout hippocampus can be displaced laterally and sometimes rostrally on this genetic background.

## Corpus callosal abnormalities in Sv129*Pas* knockout mice

Indeed, we also observed severe agenesis of the corpus callosum in Sv129*Pas* knockout mice (Fig. 6A,B). Analysis of coronal cryosections from adult knockout mice, colored with a combination of cresyl violet and luxol blue to reveal fiber tracts readily, showed an almost complete absence of callosal fibers traversing the hemispheres. The callosal fibers instead terminated close to the midline (Fig. 6B), resembling Probst bundles. The differing shape and position of the dorsal part of the hippocampus identified in Sv129*Pas* knockout animals can be explained by this abnormality, suggesting a relationship between the development of the corpus callosum and the hippocampus. This has indeed, previously been proposed to be the case in the human brain (Magee and Olson, 1961).

Agenesis of the corpus callosum has previously been documented to be present in some wild-type mice on certain backgrounds, as well as in some healthy humans (Olavarria et al., 1988; Richards et al., 2004). We therefore

Fig. 3. Hippocampal abnormalities in cases of human *DCX*-mutated type I lissencephaly. **A–C:** Nissl-stained hippocampi from a control brain at 35GW (A), compared with type I lissencephaly cases (35–36 GW) with mutations in *DCX* (B,C). Human DCX expression is normally observed throughout the Ammon's horn and in the dentate gyrus (data not shown). The two cases shown have typical and severe type I lissencephaly. The case shown in B has a DCX mutation V177E (number 148), and the case shown in C (number 207) has an R59H DCX mutation. Both cases have a hypoplastic, diffuse, and irregular Ammon's horn (I, II, III, IV) and a reduced dentate gyrus (DG), but case 207 (C) is much more severe, with an almost completely absent hippocampus and hippocampal fissure. The dentate gyrus is severely reduced (arrowhead), and it is difficult to discern both the dentate gyrus and the Ammon's horn at other rostral-caudal levels. Thus, there seems to be variability in hippocampal abnormalities among *DCX*-mutated cases. Sub, subiculum; EC, entorhinal cortex. Scale bar = 800 μm.

TABLE 1. μMRI Study[1]

| Animal | Age (months) | Hemisphere length (mm) | Agenesis | CC length (mm) | Ratio CC/hemisphere length | Hemisphere volume ($mm^3$) | Hippocamal volume ($mm^3$) | Brain weight (mg) |
|---|---|---|---|---|---|---|---|---|
| C57BL/6N WT1 | 24 | 9.56 | None | 4.3 | 0.45 | 311 | 13.5 | 450 |
| C57BL/6N *Dcx* Y/–1 | 24 | 9.94 | None | 4.41 | 0.44 | 332 | 15.5 | 470 |
| C57BL/6N WT2 | 2 | 9.38 | None | 4.19 | 0.45 | nd | 13.0 | 450 |
| C57BL/6N *Dcx* Y/–2a | 2 | 9.06 | None | 3.97 | 0.44 | nd | nd | 440 |
| C57BL/6N *Dcx* Y/–2b | 2 | 9.50 | None | 4.2 | 0.44 | nd | 13.3 | 440 |
| Sv129*Pas* WT1 | 13 | 8.81 | None | 3.67 | 0.42 | 311 | 13.7 | 460 |
| Sv129*Pas Dcx* Y/–1 | 13 | 8.94 | Complete | c.a. | — | 304 | 13.7 | 460 |
| Sv129*Pas* WT2 | 2 | 8.44 | None | 3.96 | 0.47 | nd | 14.2 | 440 |
| Sv129*Pas Dcx* +/–2 | 2 | 8.44 | Partial | 1.74 | 0.21 | nd | nd | 435 |
| Sv129*Pas Dcx* Y/–2 | 2 | 8.56 | Complete | c.a. | — | nd | 13.3 | 425 |
| C57/Sv WT | 2 | 8.63 | None | 3.91 | 0.45 | nd | nd | 450 |
| C57/Sv *Dcx* +/– | 2 | 9.06 | None | 3.76 | 0.42 | nd | nd | 470 |
| C57/Sv *Dcx* Y/– | 2 | 8.88 | None | 3.76 | 0.42 | nd | nd | 460 |

[1]c.a., Complete agenesis (although there exist some descending fibres crossing at rostral extremity); nd, not determined (extensive volume measurements in AMIRA software were performed only for selected brains); WT, wild type.

studied 10 wild-type control male mice by histology and μMRI analyses to assess the corpus callosum in the Sv129*Pas* strain (Simpson et al., 1997). We found that each wild-type mouse had a completely normal corpus callosum, strongly suggesting that the substrain of Sv129 that we use does not frequently show corpus callosum abnormalities in the wild-type state. On the other hand, we studied 10 male knockout littermate mice, and each knockout mouse had a callosal agenesis. Therefore, it seems reasonable to attribute the corpus callosum phenotype observed in the knockout animals specifically to the absence of Dcx. We did not detect any differences in other fiber structures in the acallosal mice; e.g., the anterior and posterior commissures, the optic tract, the nigrostriatal tract, the fasciculus retroflexus, the mammillothalamic tract, and the internal capsule appeared similar between the genotypes (Fig. 6A,B). Thus, major fiber abnormalities in the *Dcx* knockout seem to be restricted to the corpus callosum.

We were interested in confirming that Dcx is expressed during the period of normal development of the corpus callosum. We therefore performed immunohistochemistry experiments in wild-type newborn mouse brain and observed an expression of Dcx in the developing corpus callosum (Supplementary Fig. 7A–D). The formation of the corpus callosum in the rodent continues in the first 2 postnatal weeks (Silver et al., 1982). We therefore also performed Western blot analyses to check for Dcx expression at later postnatal stages. An expression of Dcx was observed in 4- and 10-day-old mouse brain extracts, with diminished expression at later stages (Supplementary Fig. 7E). Thus the temporal expression of Dcx is indeed in keeping with a possible role in corpus callosum development.

We performed further studies with μMRI to obtain a global view of the callosal abnormalities in the *Dcx* knockout mice compared with wild type, both on Sv129*Pas* and on C57BL/6N pure backgrounds and on the F1 Sv129*Pas*/C57BL/6N hybrid background. Similarly to the histological results, agenesis of the corpus callosum in the Sv129*Pas* knockout was clearly evident by μMRI (Table 1, Fig. 7). Heterozygote female littermate mice on this background showed a phenotype intermediate to that observed in the knockout and the control, i.e. a reduced corpus callosum (Table 1, Fig. 7B). This intermediate phenotype suggests that the degree of severity of corpus callosum abnormalities is dependent on the number of cells expressing Dcx protein. No abnormalities, even subtle abnormalities, could be detected by μMRI analyses in knockout mice on either the C57BL/6N or the Sv129*Pas*/C57BL/6N hybrid backgrounds (Table 1), suggesting a clear predisposition for this abnormality only in the Sv129*Pas* strain.

## Callosal abnormalities are more severe caudally in Sv129*Pas Dcx* Y/– mice

The crossing of callosal fibers is known to require fusion at the midline and axon guidance by correctly positioned glial structures (Richards et al., 2004). Dcx is not expressed in glial cells (Francis et al., 1999), but nevertheless we decided to verify such structures in the Sv129*Pas* strain. We were unable at E17.5 to detect any abnormalities in midline structures in wild-type and knockout brains (data not shown). By glial fibrillary acidic protein (GFAP) labeling in newborn brains, we observed that both the glial wedges and the indusium griseum glia were normal in control and mutant animals (data not shown). Neurons of the sling, another midline structure positioned directly ventral to the corpus callosum (Shu et al., 2003) and detectable by Nissl staining, do not seem different in newborn wild-type and mutant mice (data not shown). The two newborn knockout mouse brains analyzed showed some early callosal fibers crossing the midline at the rostral extremity, indistinguishable from wild type (data not shown). Combined, these data suggest that there is no structural abnormality preventing the callosal fibers at the rostral extremity crossing the midline in the Sv129*Pas* strain.

In μMRI and histological studies, we identified some variations in the corpus callosal phenotype between knockout animals (Fig. 8A–F). The most severe class of animals showed no callosal fibers crossing the midline, although, in rostral coronal slices, certain callosal fibers descended ipsilaterally toward the midline to join the fornix (Fig. 8C,F). Heterozygote mice showed an intermediate form of this phenotype (Fig. 8E). Ventrally descending fibers, though less distinct, are observed in wild-type animals, positioned rostral to sections showing the first crossing callosal fibers (between Bregma positions 1.18 mm and 1.34 mm, Franklin and Paxinos, 1997; data not shown). However, the severe class of knockout animals (n = 3) had such descending fibers across a longer rostrocaudal extent, reaching the level of the anterior commissure. In the other knockout animals analyzed, fibers

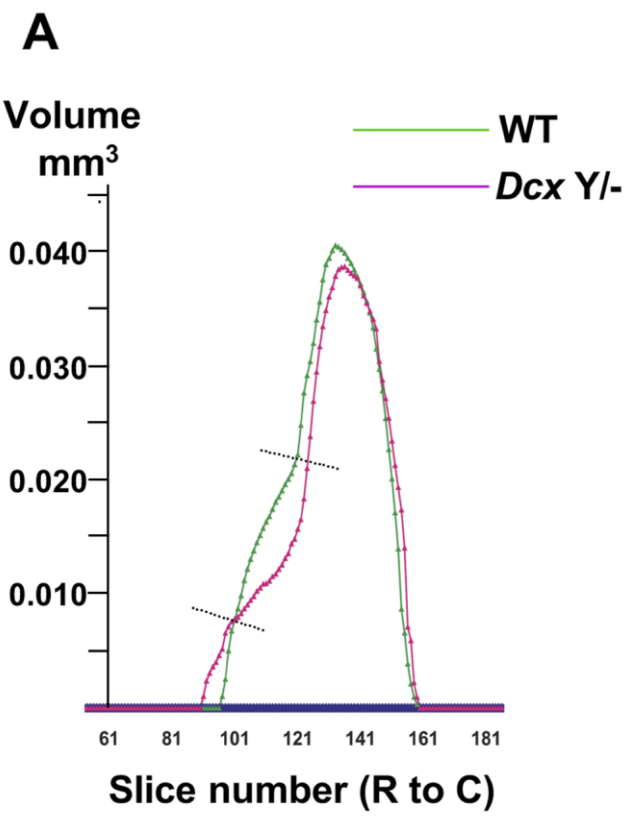


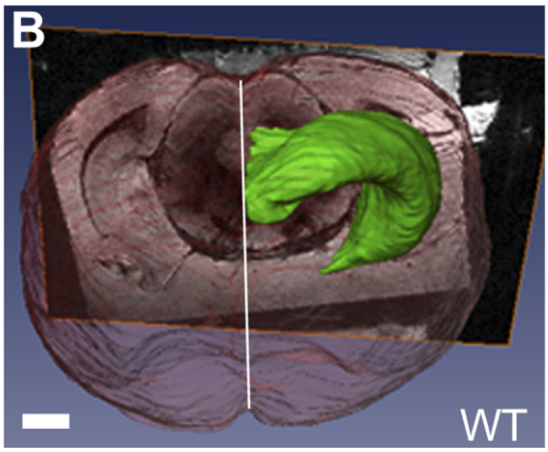


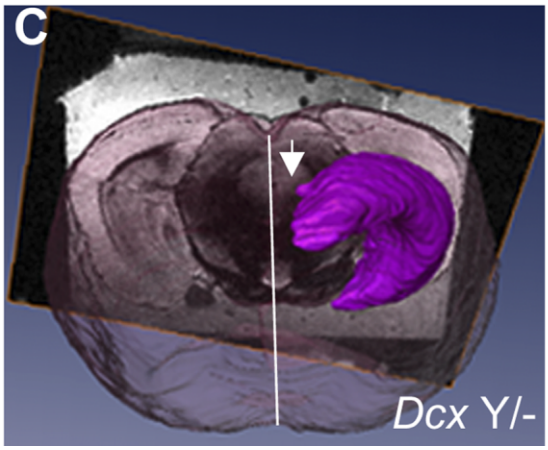


crossed the midline to variable degrees at the rostral extremity of the corpus callosum (Fig. 8B). However, all knockout animals showed a caudal agenesis. In agreement with our observations of rostral crossing fibers in two newborn mouse brains, these data suggest that the formation of the later-formed caudal part of the corpus callosum strictly requires Dcx, whereas the rostral part is able to form in its absence in some cases.

μMRI and histological analyses showed that the cingulate cortex descended more ventrally in knockout animals (Fig. 8B,C,F). In some cases, the septal nuclei appeared deformed as a consequence of these alterations (Fig. 8D–F). It seems likely therefore that the crossing callosal fibers normally limit the ventral extent of the cingulate cortex. It remains possible that abnormalities in the cingulate cortex in knockout mice reflect a primary defect contributing to the inability of callosal fibers to cross the midline. However, no differences were evident in the cingulate cortex during embryogenesis or at newborn stages (data not shown). In more caudal regions, fewer differences in other brain structures were observed, although the two hemispheres appeared more widely separated in histological sections of *Dcx* knockout brains compared with controls (data not shown).

μMRI analyses also showed that there were no differences in the thickness of the cortex between wild-type and knockout mice, suggesting that callosal neurons are correctly represented and that callosal agenesis is not associated with neuronal loss. In addition, the abnormal bundles of callosal fiber termini present at the midline in adult knockout mice suggest that axon growth per se is possible but that the final crossing steps are perturbed. Thus, Dcx, a microtubule-associated protein, often concentrated in growing neuronal processes (Francis et al., 1999; Meyer et al., 2002), seems likely to contribute to the terminal steps of callosal axon growth and guidance across the midline.

## Corpus callosal abnormalities in human patients

A previous study (Dobyns et al., 1999) reported that eight of 12 patients with known mutations in *DCX* also

Fig. 4. Position modifications of the Sv129*Pas* adult knockout hippocampus. **A:** μMRI studies of Sv129*Pas* mice allowed a calculation of the volumes of the hippocampus in each MRI slice in wild-type vs. *Dcx* Y/– mice. The graph shows the profiles of the hippocampal volumes for one pair of animals (aged 2 months), with volumes from the wild-type animal plotted in green compared with the knockout animal in pink. Comparing individual hippocampal volumes slice by slice in a rostral to caudal orientation shows that the volumes rise more slowly in the knockout compared with the control (region indicated by dotted lines). In addition, the hippocampus extends more rostrally in the knockout animal compared with the control. Differences are also observed when considering the data in sagittal sections in a medial to lateral orientation (data not shown). The differing profile in the area marked by the dotted lines corresponds to the rostrodorsal part of the hippocampus. Between slices 104 and 126, added volumes are 6.4 $mm^3$ for the wild type and 5.1 $mm^3$ for the *Dcx* Y/– hippocampus. Similar hippocampal volume profiles were obtained for a second pair of animals aged 13 months (Supplementary Fig. 5). **B,C:** Summarized data in three-dimensional representations of the hippocampi from *Dcx* Y/– and control animals (aged 13 months), observed in the coronal plane looking toward the cerebellum, show that the less voluminous dorsal part of the hippocampus is turned away from the midline (white line) in the knockout animal (abnormality indicated by arrow). Scale bar = 1,500 μm.

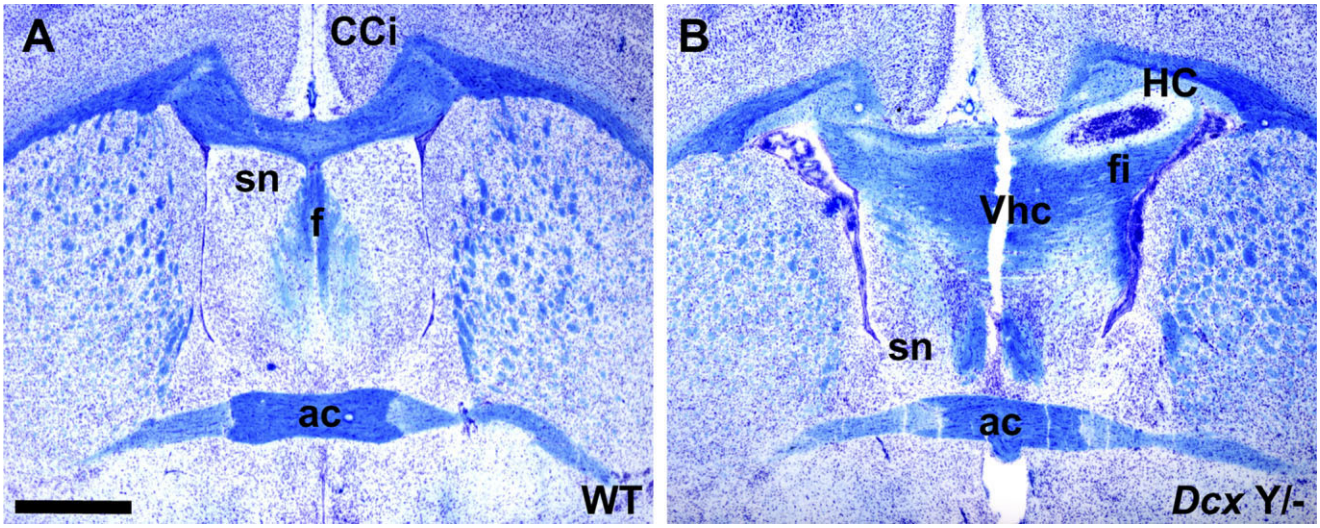


Fig. 5. Displacement of the hippocampus rostrally in some adult knockout animals. **A,B:** Cresyl violet/luxol blue- stained serial coronal sections comparing a wild-type (A) and a knockout (B) section show that a more rostrally positioned hippocampus, hippocampal fimbria (fi), and ventral hippocampal commissure (Vhc) are present in some knockout animals on the Sv129*Pas* background. CCi, cingulate cortex; sn, septal nuclei; ac, anterior commissure; f, fornix. Scale bar = 1,000 μm.

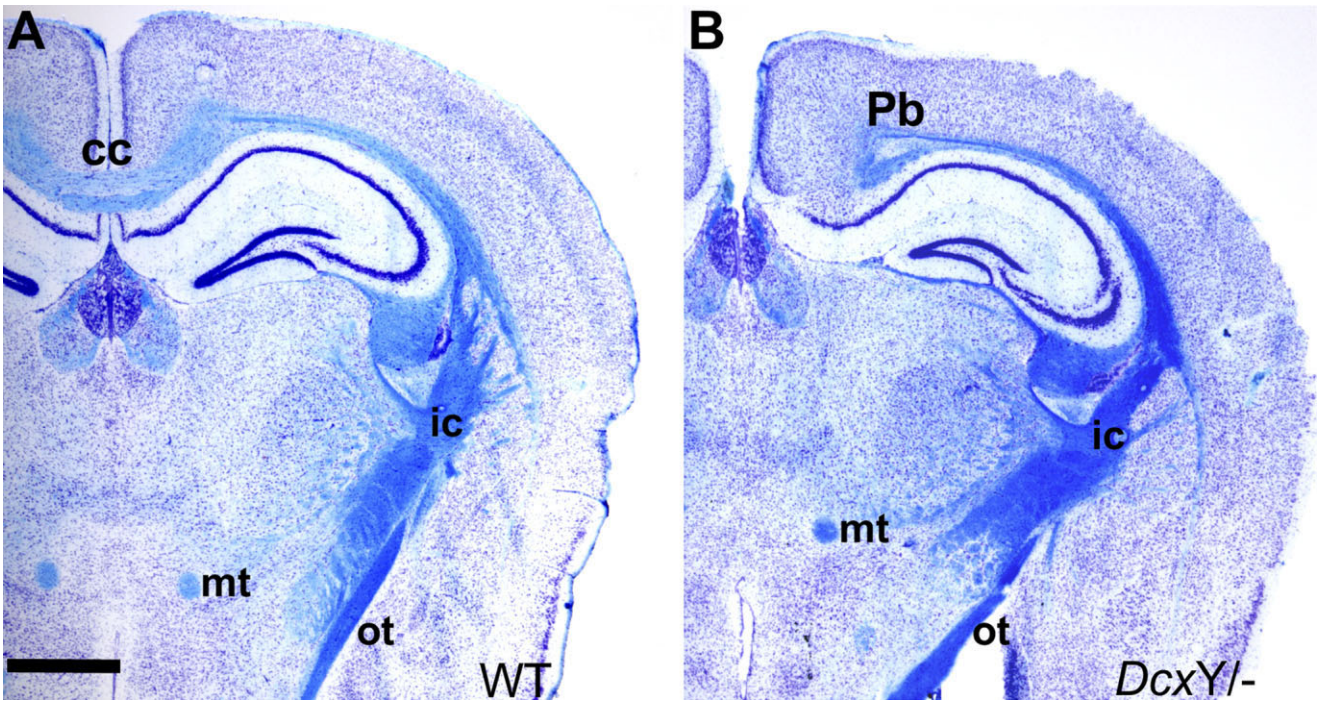


Fig. 6. Agenesis of the corpus callosum in Sv129*Pas* mutant mice. **A,B:** Cresyl violet/luxol blue-stained coronal sections from the same animals as in Figure 5 show agenesis of the corpus callosum (cc) in the male hemizygote knockout animal (B) compared with the male control animal (A), which displays callosal fibers (blue) joining the two hemispheres. Callosal fibers in the knockout animal terminate in a structure resembling a Probst bundle (Pb). Other fiber tracts, such as the internal capsule (ic), the optic tract (ot), and the mamillothalamic tract (mt), show no major differences. These combined data suggest a relationship between development of the corpus callosum and medial structures. Scale bar = 1,000 μm.

had a mild or moderate hypoplasia of the corpus callosum, with the remaining four patients noted as "unknown." We were interested in assessing the severity of abnormalities in a cohort of type I lissencephaly and subcortical laminar heterotopia (SCLH) patients for whom *DCX* mutations have been identified in our mutation screening center. Among 20 patients of variable ethnic origins, for which the state of the corpus callosum was annotated, eight were

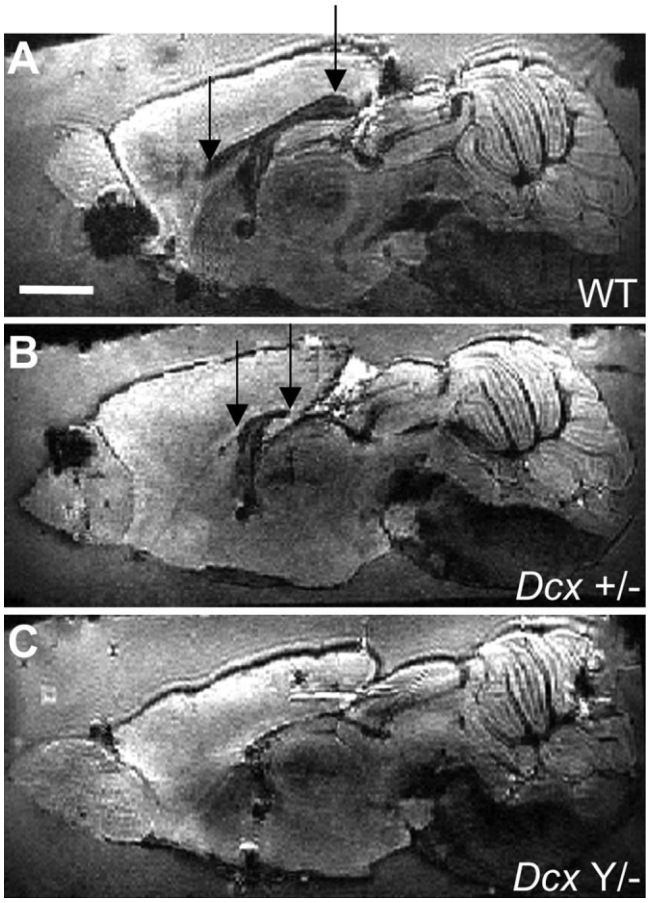


Fig. 7. Corpus callosum phenotypes in Sv129*Pas* adult knockout and heterozygote mice. **A–C:** Sagittal μMRI sections are shown from a control male adult animal (A), a littermate female heterozygote (*Dcx* +/–, B), and a littermate male knockout (*Dcx* Y/–, C). The rostral and caudal extremities of the corpus callosum are indicated by arrows. The heterozygote mouse brain shows a partial agenesis of the corpus callosum, a phenotype intermediate between the total agenesis observed in the knockout animal and the normal corpus callosum observed in the wild-type mouse. Scale bar = 1,500 μm.

reported to have abnormalities in this structure (Table 2). Six of these eight patients had the severest form of this disorder (agyria or agyria-pachygyria), suggesting a strong association between callosal abnormalities and this phenotype. Two patients with SCLH also had similar callosal abnormalities, although the majority (10/12) of these more mildly affected patients had a normal corpus callosum (Table 2).

Among the eight cases in our cohort with corpus callosum abnormalities, two showed a complete agenesis of the corpus callosum, two an abnormally thin corpus callosum, and four cases an abnormally thick corpus callosum (Fig. 9A–E). This variability was not correlated with neocortical severity (Table 2). An abnormally thick corpus callosum, the most frequently observed abnormality, was notably identified in two MRI-analyzed cases (cases 76 and 1-01, with SCLH and agyria-pachygyria, respectively) and two neurofetopathologically-analyzed cases (cases 148 and 207, both exhibiting agyria). For the latter cases, corpus callosum formation is expected to be complete at the stage analyzed (35 GW). A thick corpus callosum could therefore arise through perturbed pruning mechanisms, which are known to occur naturally for excess corpus callosum fibers at late stages of human prenatal development. Alternatively, it is also possible that fibers are less well packed compared with normal. It is not possible to distinguish between these possibilities with MRI and histological data alone. However, in the fetal case shown in Figure 9E (case 207), further examination of the corpus callosum at different rostral-caudal levels also showed a partial agenesis, giving rise to the possibility that a thickened corpus callosum might contain misguided crossing fibers destined for more rostral or caudal regions. Indeed, in this case, the genu and body of the corpus callosum were present, but the splenium, a later-formed region of the corpus callosum (Richards et al., 2004), was absent. In addition, this case showed an abnormally thick septum, apparently joined to the corpus callosum (Fig. 9E). In combination with severe hypoplasia and abnormal orientation of the hippocampus (Table 2, Fig. 3C), at least in this one *DCX*-mutated case analyzed in detail, it appears that major rostral parts of the corpus callosum are better preserved than caudal parts, and corpus callosum defects are associated with medial brain structure abnormalities.

It is noteworthy that two severely affected patients with agyria-pachygyria had an apparent corpus callosum (Fig. 9B, and data not shown), showing that neocortical abnormalities do not necessarily give rise to severe corpus callosal defects. The relative preservation of interhemispheric fibers in these patients could suggest an influence of genetic background on the callosal phenotype. Indeed, this is supported by the fact that the R186C mutation is present both in a female with no callosal abnormalities (case 4-01) and in a female with an abnormally thick corpus callosum (case 76), both of whom have thick SCLH. Thus, corpus callosum development in humans may be sensitive to genetic background, as is the case in the mouse. It still remains difficult to compare human and mouse phenotypes because of the neocortical differences; however, our combined data suggest certain parallels between human and mouse callosal development, as has been suggested by others (Magee and Olson, 1961; Richards et al., 2004).

## DISCUSSION

We identify here specific radial migration abnormalities in *Dcx* knockout mice during the development of the hippocampus, leading to a divided CA3 pyramidal cell layer in the adult. Severe corpus callosal abnormalities, revealed on the susceptible Sv129*Pas* background, segregated specifically in *Dcx* knockout mice. We found that corpus callosal and hippocampal abnormalities are common between *DCX*/*Dcx*-mutated man and mouse, although we show that the nature and severity of these abnormalities are not strictly conserved. The presence of neocortical abnormalities in human but not in mouse probably has a differential effect on the development of these structures. Nevertheless, our studies in the mouse indicate an intrinsic function for Dcx in their development, and the same may be true for human DCX.

We identified heterotopic pyramidal cell layers in the mouse hippocampus during development, first at E17.5 mainly in the CA3 region and later at E18.5 throughout the Ammon's horn. This CA3–CA1 gradient is in fact

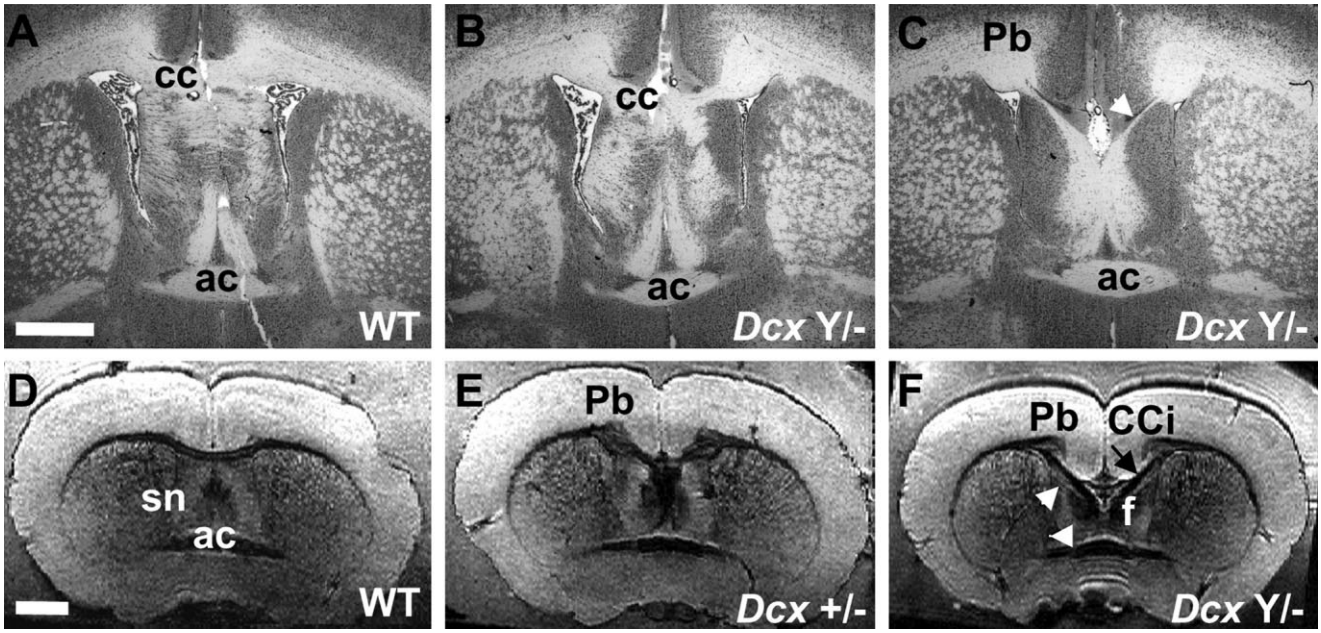


Fig. 8. Corpus callosum phenotype and associated abnormalities of Sv129*Pas* heterozygote and knockout mice. **A–C:** Histological coronal sections from one wild-type animal (A) and two knockout animals (B,C) show the variability in the knockout phenotypes. Certain knockout animals were observed to have some callosal fibers crossing the midline in rostral regions (B), with nevertheless a severe central and posterior agenesis. Other animals analyzed by cryosectioning had only descending fibers joining the fornix, with no visible fibers crossing over to the contralateral cortex (C). Such descending fibers can also be distinguished in wild-type animals, rostral to crossing corpus callosum fibers (data not shown). **D–F:** μMRI images are shown from adult littermate male control, female heterozygote, and male knockout mouse brains. Rostrally, where the anterior commissure (ac) crosses the midline, in addition to the presence of Probst bundles (Pb), rostral fibers (arrow) are observed descending toward the fornix (f) in knockout animals (F), as shown also in C by histological staining. Heterozygote animals show both Probst bundles and descending fibers (E). In addition, the cingulate cortex (CCi) seems to descend farther in the knockout compared with the control, with an intermediate phenotype observed in the heterozygote (E, F). Perhaps as a consequence of the descending cingulate cortex, the dorsal septal nuclei (sn) appear deformed (arrowheads, F). In total, 10 male knockout and 10 male wild-type animals on the Sv129*Pas* background were analyzed by either μMRI or cryosectioning. All knockout animals had a severe caudal agenesis of the corpus callosum, whereas no agenesis was detected in the wild-type animals. Scale bars = 1,000 μm in A (applies to A–C); 1,000 μm in D (applies to D–F).

TABLE 2. Callosal Abnormalities in *DCX*-Mutated Patients[1]

| Patient number | Corpus callosum | Cortical abnormality | Sex | Assessed by | DCX mutation |
|---|---|---|---|---|---|
| 9-01 | Normal | SCLH | F | MRI | p.I250T[3] |
| 15-01 | Normal | SCLH | F | MRI | p.G223E[3] |
| 17 | Normal | SCLH | F | MRI | p.K193X |
| 42 | Normal | SCLH | F | MRI | p.V177G |
| 277 | Normal | SCLH | F | MRI | p.G122W |
| 322 | Normal | SCLH | M | MRI | p.R303X |
| 283 | Normal | SCLH | F | MRI | p.T88K |
| 4-01 | Normal | SCLH | F | MRI | p.R186C[3] |
| 76 | Thick | SCLH | F | MRI | p.R186C |
| 282 | Thin | SCLH | F | MRI | p.R19X |
| 128 | Normal | SCLH + pachygyria | M | MRI | p.del VK189-190, ins YHHQ190-193 |
| 320 | Normal | Pachygyria | M | MRI | p.T203S |
| 93 | Normal | a-p | M | MRI | p.R186H |
| 192 | Normal | a-p | M | Neuropathology | p.del D248 (reduced hippocampus) |
| 1-01 (92) | Thick | a-p | M | MRI | p.D62N[3] |
| 2-01 | Thin[2] | a-p | M | MRI | p.R192W[3] |
| 11-01 (103) | c.a. | a-p | F | MRI | c.1223+1 G to A (exon 4 skipped)[3] |
| 203 | c.a. | a-p | M | MRI | p.D241Y |
| 148 | Thick | Agyria | M | Neuropathology | p.V177E (reduced hippocampus) |
| 207 | Thick | Agyria | M | Neuropathology | p.R59H (absent hippocampus) |

[1]a-p, Agyria-pachygyria; c.a., complete agenesis; p, protein; c, cDNA.
[2]Mother and sister with SCLH have normal corpus callosum.
[3]Mutations reported by des Portes et al. (1998a,b).

reminiscent of established peaks of neurogenesis for radially migrating hippocampal pyramidal neurons (Bayer, 1980; Soriano et al., 1986). A BrdU injection at E15.5 confirmed that the heterotopic cells most likely represent pyramidal cells slowed in their migration compared with wild type. A characteristic of pyramidal cell migration in the hippocampus is the fact that postmitotic migrating neurons spend several days "sojourning" in the interme-

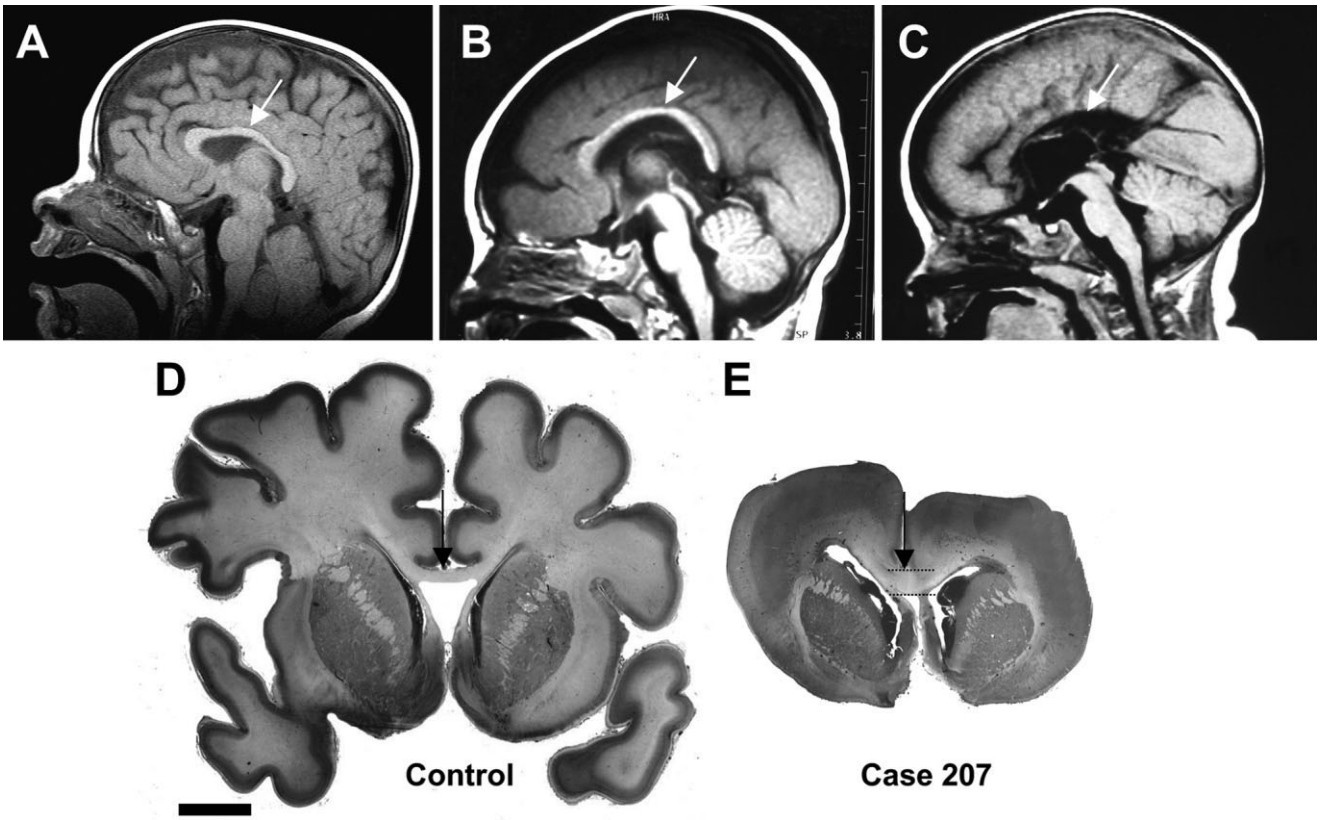


Fig. 9. Corpus callosum abnormalities in cases of human *DCX*-mutated type I lissencephaly. **A:** An MRI is shown from a normal individual aged 1 year. The corpus callosum is indicated with an arrow. **B,C:** MRIs are compared between a patient with agyria and crossing callosal fibers (B) and a patient with agyria and a complete agenesis of the corpus callosum (C, number 11-01 in Table 2). The arrow indicates the normal position of the corpus callosum. **D,E:** Brain sections from a control case (D) and a fetus with agyria (E), both at 35GW. The agyric fetus (number 207 in Table 2) showed an abnormally thick corpus callosum, which is twice the thickness observed in an age-matched control. As summarized in Table 2, a thick corpus callosum was found to be associated with SCLH, agyria-pachygyria, or complete agyria. In the case shown, the genu and main body of the corpus callosum were present, although the splenium and rostrum were absent (data not shown). In addition, this case showed a clearly thickened septum compared with the control. Scale bar = 10,000 μm.

diate zone (Altman and Bayer, 1990). Our data might suggest that *Dcx* knockout cells pause for longer than control cells, although the reasons for this are currently unknown. In early postnatal stages, the CA1 heterotopic band was reduced and already discontinuous with the abnormalities in the CA3 region. In the adult, the CA1 region appears largely normal, as analyzed on two genetic backgrounds. Thus, our data fit with a gradual disappearance of heterotopic CA1 cells with time. However, a large proportion of CA3 pyramidal neurons remains permanently grouped in a heterotopic band outside the normal pyramidal cell layer. These defects therefore distinguish pyramidal cell migration in the CA3 from the CA1 region. It will now be interesting to perform in-depth electrophysiological and behavioral studies to characterize these heterotopic CA3 neurons functionally.

By comparison, adult *p35*(–/–), *ApoER2*(–/–), and *Kif2a*(–/–) mice show disorganized heterotopia in both the CA1 and the CA3 regions (Wenzel et al., 2001; Trommsdorff et al., 1999; Homma et al., 2003). Notably, *reeler* and *Lis1* +/– mice show severe disruptions of the CA1 region, with a comparatively less severely affected CA3 region (Deller et al., 1999; Fleck et al., 2000; Niu et al., 2004). The CA1 region in these latter mice seems divided into several layers, resembling the defect observed in the CA3 region of *Dcx* knockout mice. It is noteworthy that all three murine lissencephaly models (*Dcx*, *Lis1*, and *reeler*) consistently show hippocampal lamination defects, despite the absence of major neocortical abnormalities in the case of *Dcx* and *Lis1* (Hirotsune et al., 1998; Cahana et al., 2001; Gambello et al., 2003). Development of the hippocampus in mouse is clearly a highly regulated process requiring different factors for the specification of the various hippocampal fields (Tole and Grove, 2001) and involving different essential proteins for CA1 vs. CA3 radial migration.

For *DCX* patients, our data show that the hippocampal phenotype is more drastic than in the mouse. A general, severe hypoplasia was observed throughout the CA regions and in the dentate gyrus, and these structures were abnormally organized. However, heterotopic neurons were not obvious at the stages examined, and CA3 did not appear to be more severely affected than other hippocampal regions. The hypoplasia was variably severe in the different cases, which might be explained by the type of mutation or alternatively by the genetic background. This more severe phenotype in human may be a consequence of the additional severe neocortical abnormalities or alterna-

tively of a more direct involvement of human DCX in the correct development of the entire Ammon's horn and the dentate gyrus. Thus, DCX could have more widespread functions in the human hippocampus, affecting both the generation and the migration of pyramidal and granule cells. Our combined results in humans and knockout mice indicate a direct role for DCX in hippocampal pyramidal cell migration.

We performed μMRI and histological analyses in *Dcx* knockout mice to characterize corpus callosal abnormalities identified on the Sv129*Pas* background. To our knowledge, this is the first μMRI study in rodent that characterizes corpus callosum agenesis on different genetic backgrounds and the anatomical variations associated with this phenotype. Acallosal "wild-type" mice have been observed on certain genetic backgrounds (Wahlsten, 1982a). However, in male wild-type mice of the Sv129*Pas* strain used in this study, no corpus callosum abnormalities were observed. It is nevertheless likely that Sv129*Pas* wild-type mice have a predisposition to corpus callosum agenesis, which is a complex multigenic phenotype (Wahlsten, 1982b). In our studies, agenesis of the corpus callosum segregated specifically with mutated *Dcx* (10/10 knockout animals analyzed). Therefore, the inactivation of *Dcx* on this background is perhaps a final trigger leading to a severe and fully penetrant agenesis. For the Sv129*Pas*/C57BL/6N F1 hybrid background, recessive mutations in the Sv129*Pas* strain (Wahlsten, 1982b) are probably compensated for by the C57BL/6N background. Thus, even in the absence of Dcx, the contribution of the C57BL/6N background is sufficient to restore the necessary factors for midline crossing. Our data therefore support a specific contributing role for Dcx in corpus callosum development, revealed under particular genetic conditions.

Acallosal *Dcx* knockout mice also showed an abnormal position and form of the dorsal part of the hippocampus. No other major developmental defects were obvious, so it seems likely that the callosal agenesis directly affects hippocampal positioning in these mice. These combined callosal and hippocampal defects could lead to learning and memory deficits in these animals. In acallosal human patients without neocortical abnormalities, the hippocampus is also abnormally oriented and sometimes hypoplastic (C. Fallet-Bianco, unpublished; Baker and Barkovich, 1992; Sato et al., 2001; Küker et al., 2002). Thus, although hippocampal position is not identical between mouse and man, it nevertheless appears that the corpus callosum, with its associated dorsal hippocampal commissure (Küker et al., 2002), is strictly required for correct hippocampal positioning in both cases.

An interesting aspect of the *Dcx* callosal phenotype is that, in some animals, fibers appear to cross at the rostral extremity of the corpus callosum. Thus, two newborn knockout mice analyzed were found to be indistinguishable from newborn wild-type mice, which at this stage have crossing fibers at the rostral extremity. Hence, it appears that an absence of Dcx might not be essential for early crossing pioneer fibers (Koester and O'Leary, 1994; Richards et al., 2004). In addition, some adult knockout mice also showed crossing fibers in rostral regions, further suggesting that early steps of callosal development occur normally. Other *Dcx* knockout animals, however, showed only an ipsilateral descent of rostral fibers along the midline. It is not yet clear whether these latter animals have lost rostral crossing fibers or whether examination of a larger number of newborn knockout animals would also show some animals with an early rostral callosal agenesis, and this remains to be further investigated. Recently reported double-knockout mice for *Dcx* and *Dclk1* were also described to have callosal agenesis, with some rostral crossing fibers (Deuel et al., 2006). These data once again point to the specificity of the phenotype that we observe on the Sv129*Pas* background in the absence of Dcx alone. In our single-knockout mice, small Probst bundles were evident across the rostral-caudal extent of the corpus callosum. These abnormalities suggest that a large proportion of Dcx-deficient corpus callosal fibers grows correctly toward the midline, but these fibers are perhaps unable to respond correctly to the appropriate guidance factors to allow them to cross over to the contralateral hemisphere. Indeed, corpus callosum abnormalities have been previously identified in a number of other pathological mouse models affecting proteins known to be involved in axon growth or guidance (*L1-CAM*, Demyanenko et al., 1999; *p35*, Kwon et al., 1999; *EphA5*, Hu et al., 2003; *EphB3*, Mendes et al., 2006; *Emx-1*, Qiu et al., 1996; *netrin*, Serafini et al., 1996; *Dcc*, Fazeli et al., 1997). Thus, loss of Dcx in mouse may perturb the final stages of axonal growth or guidance. A thickened corpus callosum in human patients, possibly containing misplaced fibers, might further support this hypothesis.

We found a variety of corpus callosum abnormalities in human patients ranging from complete agenesis to an abnormally thin or thick corpus callosum. It is noteworthy that, although we observe a tendency for severely affected type I lissencephaly patients (agyria or agyria-pachygyria cases) to show corpus callosum defects, which supports a role for neocortical abnormalities in this phenotype, smaller numbers of patients with similarly severe forms of the disease apparently show fewer defects, in that they have crossing interhemispheric fibers of normal thickness and rostral-caudal length. Thus, neocortical agyria alone does not give rise to callosal agenesis. Also, some patients with milder neocortical abnormalities (SCLH) show equally severe callosal abnormalities. In humans, as in mice, genetic background is likely to play an important role in the characteristics of these abnormalities, which complicates the interpretation of these data. This is suggested by two patients with the same mutation, both exhibiting similar forms of SCLH, with only one patient showing callosal defects. Nevertheless, the high proportion of patients with linked callosal defects and lissencephaly (six of eight patients in our study and eight of 12 patients studied by Dobyns et al., 1999) suggests a strong association between mutated DCX and callosal defects. These combined data suggest that, in addition to the influence of neocortical abnormalities, DCX could also play an intrinsic role in human corpus callosum fiber development, revealed on certain genetic backgrounds.

Our studies in the mouse pinpoint some potentially conserved roles for human and mouse DCX/Dcx in hippocampal and corpus callosal development. The severity of the human phenotype suggests that the role of DCX/Dcx in other brain structures, such as the neocortex, might have evolved greatly since the divergence of rodent and primate lineages. Ongoing studies of primate and rodent DCX/Dcx will shed further light on these evolutionary processes.

## ACKNOWLEDGMENTS

Patients and clinicians are gratefully acknowledged for supporting this work. We are also particularly grateful to Marika Nosten-Bertrand, Pascale Marcorelles, Vincent desPortes, Hilde van Esch, Catherine Daumas-Duport, and members of Jamel Chelly's laboratory for their contributions to this work. The authors thank Pierre Billuart and Thierry Bienvenu for their helpful comments on the manuscript. We gratefully acknowledge Patrick Charnay's laboratory for the use of their low-magnification microscopy facilities. This work was supported in part by grants from the French Ministère de la Recherche [Developmental Biology (to F.F.) and Neuroscience (to M.D.) sections and a PhD grant (to C.K.)] and the Fédération pour la Recherche sur le Cerveau. The contribution of the Région Ile de France to the Institut Cochin animal care facility is also acknowledged.

## LITERATURE CITED

Altman J, Bayer SA. 1990. Prolonged sojourn of developing pyramidal cells in the intermediate zone of the hippocampus and their settling in the stratum pyramidale. J Comp Neurol 301:343–364.

Baker LL, Barkovich AJ. 1992. The large temporal horn: MR analysis in developmental brain anomalies versus hydrocephalus. AJNR Am J Neuroradiol 13:115–22.

Banbury Conference on Genetic Background. 1997. Mutant mice and neuroscience: recommendations concerning genetic background. Neuron 19:755–759.

Bayer SA. 1980. Development of the hippocampal region in the rat. I. Neurogenesis examined with $^{3}$H-thymidine autoradiography. J Comp Neurol 190:87–114.

Cahana A, Escamez T, Nowakowski RS, Hayes NL, Giacobini M, von Holst A, Shmueli O, Sapir T, McConnell SK, Wurst W, Martinez S, Reiner O. 2001. Targeted mutagenesis of Lis1 disrupts cortical development and LIS1 homodimerization. Proc Natl Acad Sci U S A 98:6429–6434.

Corbo J, Deuel T, Long J, LaPorte P, Tsai E, Wynshaw-Boris A, Walsh C. 2002. Doublecortin is required in mice for lamination of the hippocampus but not the neocortex. J Neurosci 22:7548–7557.

Delatour B, Guegan M, Volk A, Dhenain M. 2006. In vivo MRI and histological evaluation of brain atrophy in APP/PS1 transgenic mice. Neurobiol Aging (in press).

Deller T, Drakew A, Heimrich B, Forster E, Tielsch A, Frotscher M. 1999. The hippocampus of the reeler mutant mouse: fiber segregation in area CA1 depends on the position of the postsynaptic target cells. Exp Neurol 156:254–267.

Demyanenko GP, Tsai AY, Maness PF. 1999. Abnormalities in neuronal process extension, hippocampal development, and the ventricular system of L1 knockout mice. J Neurosci 19:4907–4920.

des Portes V, Pinard JM, Billuart P, Vinet MC, Koulakoff A, Carrié A, Gelot A, Dupuis E, Motte J, Berwald-Netter Y, Catala C, Kahn A, Beldjord C, Chelly J. 1998a. Identification of a novel CNS gene required for neuronal migration and involved in X-linked subcortical laminar heterotopia and lissencephaly syndrome. Cell 92:51–61.

des Portes V, Francis F, Pinard J-P, Desguerre I, Moutard M-L, Snoeck I, Meiners LC, Capron F, Cusmai R, Ricci S, Motte J, Echenne B, Ponsot G, Dulac O, Chelly J, Beldjord C. 1998b. doublecortin is the major gene causing X-linked subcortical laminar heterotopia (SCLH). Hum Mol Gen 7:1063–1070.

Deuel TA, Liu JS, Corbo JC, Yoo SY, Rorke-Adams LB, Walsh CA. 2006. Genetic interactions between doublecortin and doublecortin-like kinase in neuronal migration and axon outgrowth. Neuron 49:41–53.

Dhenain M, Ruffins SW, Jacobs RE. 2001. Three dimensional digital mouse atlas using high resolution MRI. Dev Biol 232:458–470.

Dhenain M, Delatour B, Walczak C, Volk A. 2006. Passive staining: a novel ex vivo MRI protocol to detect amyloid deposits in mouse models of Alzheimer's disease. Magn Reson Med 55:687–693.

Dobyns WB, Truwit CL, Ross ME, Matsumoto N, Pilz DT, Ledbetter DH, Gleeson JG, Walsh CA, Barkovich AJ. 1999. Differences in the gyral pattern distinguish chromosome 17-linked and X-linked lissencephaly. Neurology 53:270–277.

Fazeli A, Dickinson SL, Hermiston ML, Tighe RV, Steen RG, Small CG, Stoeckli ET, Keino-Masu K, Masu M, Rayburn H, Simons J, Bronson RT, Gordon JI, Tessier-Lavigne M, Weinberg RA. 1997. Phenotype of mice lacking functional deleted in colorectal cancer (Dcc) gene. Nature 386:796–804.

Fleck MW, Hirotsune S, Gambello MJ, Phillips-Tansey E, Suares G, Mervis RF, Wynshaw-Boris A, McBain CJ. 2000. Hippocampal abnormalities and enhanced excitability in a murine model of human lissencephaly. J Neurosci 20:2439–2450.

Forman MS, Squier W, Dobyns WB, Golden JA. 2005. Genotypically defined lissencephalies show distinct pathologies. J Neuropathol Exp Neurol 64:847–857.

Francis F, Koulakoff A, Chafey P, Vinet M-C, Schaar B, Boucher D, Reiner O, Kahn A, Denoulet P, McConnell SK, Berwald-Netter Y, Chelly J. 1999. Doublecortin is a developmentally regulated, microtubule-associated protein expressed in migrating neurons. Neuron 23:247–256.

Franklin KBJ, Paxinos G. 1997. The mouse brain in stereotaxic coordinates. San Diego: Academic Press.

Gambello MJ, Darling DL, Yingling J, Tanaka T, Gleeson JG, Wynshaw-Boris A. 2003. Multiple dose-dependent effects of Lis1 on cerebral cortical development. J Neurosci 23:1719–1729.

Gleeson JG, Allen KM, Fox JW, Lamperti ED, Berkovic S, Scheffer I, Cooper EC, Dobyns WB, Minnerath SR, Ross ME, Walsh CA. 1998. Doublecortin, a brain-specific gene mutated in human X-linked lissencephaly and double cortex syndrome, encodes a putative signaling. Cell 92:63–72.

Gleeson JG, Lin PT, Flanagan LA, Walsh CA. 1999. Doublecortin is a microtubule-associated protein and is expressed widely by migrating neurons. Neuron 23:257–271.

Hirotsune S, Fleck MW, Gambello MJ, Bix GJ, Chen A, Clark GD, Ledbetter DH, McBain CJ, Wynshaw-Boris A. 1998. Graded reduction of Pafah1b1 (Lis1) activity results in neuronal migration defects and early embryonic lethality. Nat Genet 19:333–339.

Homma N, Takei Y, Tanaka Y, Nakata T, Terada S, Kikkawa M, Noda Y, Hirokawa N. 2003. Kinesin superfamily protein 2A (KIF2A) functions in suppression of collateral branch extension. Cell 114:229–239.

Horesh D, Sapir T, Francis F, Grayer Wolf S, Caspi M, Elbaum M, Chelly J, Reiner O. 1999. Doublecortin, a stabilizer of microtubules. Hum Mol Gen 8:1599–1610.

Hu Z, Yue X, Shi G, Yue Y, Crockett DP, Blair-Flynn J, Reuhl K, Tessarollo L, Zhou R. 2003. Corpus callosum deficiency in transgenic mice expressing a truncated ephrin-A receptor. J Neurosci 23:10963–10970.

Kappeler C, Saillour Y, Baudoin JP, Tuy FP, Alvarez C, Houbron C, Gaspar P, Hamard G, Chelly J, Metin C, Francis F. 2006. Branching and nucleokinesis defects in migrating interneurons derived from doublecortin knockout mice. Hum Mol Genet 15:1387–1400.

Koester SE, O'Leary DD. 1994. Axons of early generated neurons in cingulate cortex pioneer the corpus callosum. J Neurosci 14:6608–6620.

Koizumi H, Higginbotham H, Poon T, Tanaka T, Brinkman BC, Gleeson JG. 2006a. Doublecortin maintains bipolar shape and nuclear translocation during migration in the adult forebrain. Nat Neurosci 9:779–786.

Koizumi H, Tanaka T, Gleeson JG. 2006b. Doublecortin-like kinase functions with doublecortin to mediate fiber tract decussation and neuronal migration. Neuron 49:55–66.

Küker W, Mayrhofer H, Mader I, Nägele T, Krägeloh-Mann I. 2003. Malformations of the midline commissures: MRI findings in different forms of callosal dysgenesis. Eur Radiol 13:598–604.

Kwon YT, Tsai LH, Crandall JE. 1999. Callosal axon guidance defects in p35(–/–) mice. J Comp Neurol 415:218–229.

Magee KR, Olson RN. 1961. The effect of absence of the corpus callosum on the position of the hippocampus and on the formation of Probst's bundle. J Comp Neurol 117:371–382.

Mendes SW, Henkemeyer M, Liebl DJ. 2006. Multiple Eph receptors and B-class ephrins regulate midline crossing of corpus callosum fibers in the developing mouse brain. J Neurosci 26:882–892.

Meyer G, Perez-Garcia CG, Gleeson JG. 2002. Selective expression of doublecortin and LIS1 in developing human cortex suggests unique modes of neuronal movement. Cereb Cortex 12:1225–1236.

Montenegro MA, Kinay D, Cendes F, Bernasconi A, Bernasconi N, Coan AC, Li LM, Guerreiro MM, Guerreiro CAM, Lopes-Cendes I, Andermann E, Dubeau F, Andermann F. 2006. Patterns of hippocampal abnormalities in malformations of cortical development. J Neurol Neurosurg Psychiatry 77:367–371.

Niu S, Renfro A, Quattrocchi CC, Sheldon M, D'Arcangelo G. 2004. Reelin promotes hippocampal dendrite development through the VLDLR/ApoER2-Dab1 pathway. Neuron 41:71–84.

Olavarria J, Serra-Oller MM, Yee KT, Van Sluyters RC. 1988. Topography of interhemispheric connections in neocortex of mice with congential deficiencies of the callosal commissure. J Comp Neurol 270:575–590.

Qiu M, Anderson S, Chen S, Meneses JJ, Hevner R, Kuwana E, Pedersen RA, Rubenstein JL. 1996. Mutation of the Emx-1 homeobox gene disrupts the corpus callosum. Dev Biol 178:174–178.

Richards LJ, Plachez C, Ren T. 2004. Mechanisms regulating the development of the corpus callosum and its agenesis in mouse and human. Clin Genet 66:276–289.

Sambrook J, Fritsch EF, Maniatis T. 1989. Molecular cloning: a laboratory manual, 2nd ed. Cold Spring Harbor, NY: Cold Spring Harbor Laboratory.

Sato N, Hatakeyama S, Shimizu N, Hikima A, Aoki J, Endo K. 2001. MR evaluation of the hippocampus in patients with congenital malformations of the brain. AJNR Am J Neuroradiol 22:389–393.

Serafini T, Colamarino SA, Leonardo ED, Wang H, Beddington R, Skarnes WC, Tessier-Lavigne M. 1996. Netrin-1 is required for commissural axon guidance in the developing vertebrate nervous system. Cell 87: 1001–1014.

Shu T, Li Y, Keller A, Richards LJ. 2003. The glial sling is a migratory population of developing neurons. Development 130:2929–2937.

Silver J, Lorenz SE, Wahlsten D, Coughlin J. 1982. Axonal guidance during development of the great cerebral commissures: descriptive and experimental studies, in vivo, on the role of preformed glial pathways. J Comp Neurol 210:10–29.

Simpson EM, Linder CC, Sargent EE, Davisson MT, Mobraaten LE, Sharp JJ. 1997. Genetic variation among 129 substrains and its importance for targeted mutagenesis in mice. Nat Genet 16:19–27.

Soriano E, Cobas A, Fairen A. 1986. Asynchronism in the neurogenesis of GABAergic and non-GABAergic neurons in the mouse hippocampus. Brain Res 395:88–92.

Tole S, Grove EA. 2001. Detailed field pattern is intrinsic to the embryonic mouse hippocampus early in neurogenesis. J Neurosci 21:1580–1589.

Trommsdorff M, Gotthardt M, Hiesberger T, Shelton J, Stockinger W, Nimpf J, Hammer RE, Richardson JA, Herz J. 1999. Reeler/Disabled-like disruption of neuronal migration in knockout mice lacking the VLDL receptor and ApoE receptor 2. Cell 97:689–701.

Wahlsten D. 1982a. Deficiency of corpus callosum varies with strain and supplier of the mice. Brain Res 239:329–347.

Wahlsten D. 1982b. Mode of inheritance of deficient corpus callosum in mice. J Hered 73:281–285.

Wenzel HJ, Robbins CA, Tsai LH, Schwartzkroin PA. 2001. Abnormal morphological and functional organization of the hippocampus in a p35 mutant model of cortical dysplasia associated with spontaneous seizures. J Neurosci 21:983–998.